Supporting Information

A Multi-Rotor Near-Infrared Probe for High-Sensitivity Imaging of Mitochondrial Viscosity in Epilepsy

Pengpeng Lu, [a] Yuening Wang, [a] Yan Huang, * [b] and Limin Zhang* [a]

[a] School of Chemistry and Molecular Engineering, East China Normal University, Dongchuan Road 500, Shanghai 200241, China.

[b] School of Pharmacy, Binzhou Medical University, Yantai 264003, China

Table of Contents

1. Experimental Section

2. Synthesis and characterization of Cy-TPE.

3. Performance Evaluation of Cy-TPE.

4. Behavioral assessments.

5. References

1. Experimental Section

Instruments. The ^{1}H NMR and ^{13}C NMR spectra were obtained from a 600 MHz Bruker NMR spectrometer (Bruker, Germany). The mass spectrum was detected by a Bruker ESI time-of-flight MS system (Bruker, Germany). The fluorescence spectrum and the UV-vis absorption spectrum were recorded by using a Hitachi F-4500 fluorescence spectrometer (Hitachi, Japan) and a Hitachi UH-5300 spectrometer (Hitachi, Japan), respectively. Fluorescence imaging was performed using a Leica Stellaris 8 STED confocal scanning microscope (Leica Microsystems, Germany) equipped with a Living Cell Workstation (STXF, TOKAI HIT). The cytotoxicity assays were measured by Varioskan LUX multimode microplate reader (Thermo Fisher scientific, USA). The JC-1 assay was carried out by a FACS Calibur flow cytometry (Becton, Dickinson and Company, USA). The fresh mouse brain tissue slices were obtained using a Leica VT3000 vibrating-blade microtome (Germany) with a thickness of about 300 μm.

Computational Details. The theoretical calculations were performed using the Gaussian 16 suite of package. The structures of the studied molecules were fully optimized at the B3LYP-D3BJ/6-31G (d, p) level of theory. For time-dependent density-functional theory (TD-DFT) calculations, the excitation optimized structure was obtained using the CAM-B3LYP method (CAM-B3LYP/6-31G (d, p)). The highest occupied orbital (HOMO) and lowest unoccupied orbital (LUMO) orbitals were calculated and analyzed using Multiwfn software, [S1] and the isosurfaces were visualized using the Visual Molecular Dynamics (VMD) program. [S2]

Primary Neuronal Culture. The isolation and culture of cortical neurons followed an established protocol. Briefly, newborn C57BL/6 wild-type mice (within 24 h of birth) were anesthetized with halothane, and the brains were rapidly dissected into ice-cold HBSS. Cortical tissues were carefully isolated and digested with papain at 37 °C for 12 minutes. After enzymatic digestion, the tissues were gently triturated and plated onto poly-D-lysine-coated 35 mm Petri dishes at a density of 1×10^6 cells per dish. Neurons were maintained in neurobasal medium supplemented with L-glutamine and B27, with the medium refreshed three times per week. Cultures were incubated at 37 °C in a humidified atmosphere containing 5% CO_2. After 7 days in vitro, the neurons were ready for subsequent imaging experiments.

Cytotoxicity and Apoptosis Assays. The cytotoxicity assays were measured by Cell Counting Kit-8 (CCK-8). Neurons in 96-well plates were incubated with different concentrations of the Cy-TPE probe (0, 10, 20, 30, 40, 50 and 60 μM) and cultured for 24 h. Then, the neurons in each well were treated with 10 μL CCK-8 solution and further continuously incubated for 1 h at 37 °C. After that, absorbance was measured at 450 nm in a Varioskan LUX multimode microplate reader (Thermo Fisher scientific, USA). Cell viability was defined as the ratio of absorbance in the experimental groups to that in the blank control groups.

Establishment of Acute Seizure Model and *In Vivo* Imaging. An acute seizure model was established in adult male C57BL/6J mice (6-8 weeks) by intraperitoneal administration of kainic acid (KA; 20 mg/kg in saline).[S3] Animals that progressed to Racine stage 4 or 5 seizures, including status epilepticus, within a 30-minute observation window were included in subsequent procedures. For control animals, an equal volume of saline was administered. For in vivo imaging, epileptic mice were anesthetized and placed in a stereotaxic apparatus. The Cy-TPE probe (1 μL, 20 μM in saline) was microinjected into the left hippocampus at a rate of 0.2 μL/min. After injection, the

needle was left in place for an additional 5 minutes to prevent backflow. Fluorescence imaging was performed using an in vivo imaging system with a 680 nm excitation laser, and the emission signal was captured using a 725 ± 30 nm bandpass filter. All animal procedures were approved by the Institutional Animal Care and Use Committee of East China Normal University.

KA-induced acute seizure model. Mice that developed status epilepticus (SE) following KA administration were included in the study. SE was defined as continuous seizure activity lasting longer than 10 minutes, characterized by recurrent seizure episodes (stages 1–5) occurring at intervals of less than 1 minute. Seizure behavior was scored according to the Racine scale: stage 0, no response; stage 1, staring and reduced locomotion; stage 2, head nodding; stage 3, unilateral forelimb clonus; stage 4, bilateral forelimb clonus; stage 5, rearing and falling; and stage 6, status epilepticus and death. In addition to recording seizure scores, overall seizure severity was quantified for each mouse by integrating the scores over the entire observation period. Hippocampal tissues were collected 24 hours after KA treatment for subsequent analysis.

Preparation and imaging of mouse brain tissue slices. All animal experiments were performed according to the guidelines of the Care and Use of Laboratory Animals formulated by the Ministry of Science and Technology of China and were approved by the Animal Care and Use Committee of East China Normal University (approval no. m20251007, Shanghai, China). Five-month-old normal mice were purchased from the Laboratory Animal Center of the Chinese Academy of Science. First, the fresh mouse brain tissue slices were obtained using a Leica VT3000 vibrating-blade microtome (Germany) with a thickness of about 300 μm. This step was fully operated in ice cold artificial cerebrospinal fluid (ACSF, NaCl 124.0 mM, KCl 3.0 mM, $NaHCO_3$ 26.0 mM, NaH_2PO_4 1.24 mM, $MgSO_4$ 8.0 mM, $CaCl_2$ 0.1 mM and D-glucose 10.0 mM) under a 95% O_2 and 5% CO_2 atmosphere. Second, the slices were transferred to an incubation chamber filled with ACSF containing 30.0 μM Cy-TPE at 37 ℃ for 60 min, and the ACSF was aerated with 95% O_2 and 5% CO_2. The treated slices were then washed with ACSF at least three times for imaging.

Histology study. After the above experiments, mice were deeply anesthetized with Pelltobarbitalum Natricum (40 mg/kg, i.p.) and perfused transcardially with 0.1 M PBS followed by 4% paraformaldehyde in 0.1 M PBS. Coronal brain sections (a thickness of 20 μm) were blocked with 10% horse serum and 0.5% Triton X-100 in PBS, and then incubated with antibodies to NeuN, GFAP. After washing with PBS, sections were incubated with secondary antibodies and DAPI. Sections were washed, mounted, and imaged using Zeiss LSM780 confocal microscope (Jena, Germany). ImageJ software was used to count NeuN- and GFAP-positive cells. At least three regions from each section and three sections were imaged for each animal, and three animals were used for each group.

2. Synthesis and characterization of Cy-TPE.

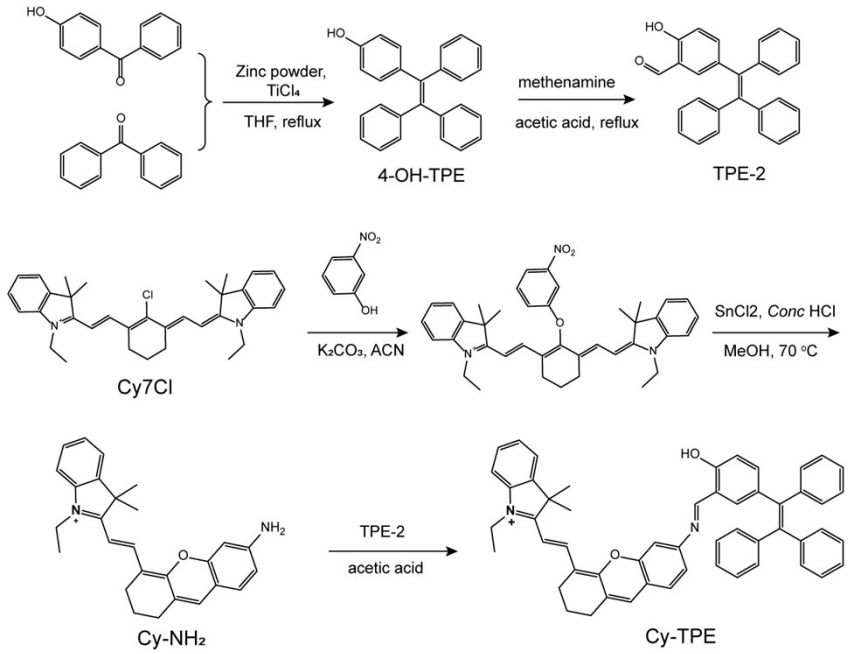

Scheme S1. The synthesis procedures of Cy-TPE.

Synthesis of compound TPE-2. TPE-2 was synthesized according to a literature procedure.[S4] 4-OH-TPE (3.482 g, 10 mmol) and methenamine (2.102 g, 1.5 eq.) were refluxed in 100 mL acetic acid for 3 h. Then, the reaction solution was poured into ice water and extracted with CH_2Cl_2. The combined organic solution was concentrated under reduced pressure. After purification by silica gel chromatography (petroleum ether / CH_2Cl_2, 5:1, v/v), TPE-2 was obtained as an orange-yellow solid in 35% yield. ^{1}H NMR (600 MHz, Chloroform-*d*) δ 10.99 (s, 1H), 9.62 (s, 1H), 7.25 (s, 2H), 7.20 – 7.17 (m, 6H), 7.15 (d, *J* = 2.2 Hz, 3H), 7.13 – 7.10 (m, 4H), 7.08 (dd, *J* = 6.7, 3.0 Hz, 2H), 6.78 (d, *J* = 9.3 Hz, 1H). ^{13}C NMR (150 MHz, $CDCl_3$) δ 196.63, 160.26, 143.45, 143.42, 143.13, 141.56, 140.19, 138.96, 136.51, 135.72, 131.43, 131.35, 131.31, 128.14, 128.03, 127.84, 126.93, 126.89, 126.73, 120.24, 117.05.

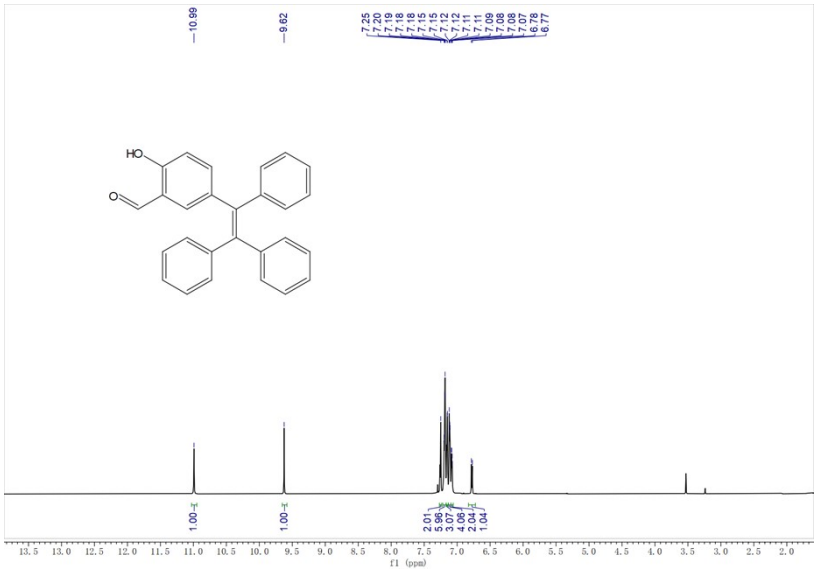

Fig. S1. ^{1}H NMR spectrum of TPE-2.

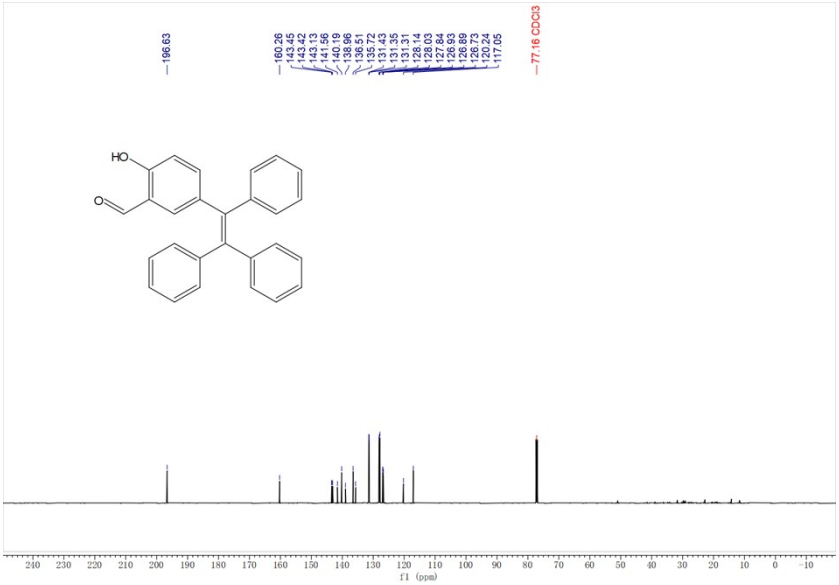

Fig. S2. ^{13}C NMR spectrum of TPE-2.

Synthesis of compound Cy-NH_2. Cy-NH_2 was synthesized according to a literature procedure.[S5] The key intermediate CY-NH_2 (277 mg) was prepared with Cy7Cl (639 mg, 1.0 mmol) and 3-nitrophenol (347 mg, 2.5 mmol) as starting materials and purified by column chromatography (DCM/MeOH = 40/1 to 5/1, v/v) in 50.8% yield. ^{1}H NMR (600 MHz, Methanol-d_4) δ 8.65 (d, J = 14.3 Hz, 1H), 7.56 (d, J = 10.1 Hz, 2H), 7.49 – 7.42 (m, 1H), 7.36 (d, J = 8.5 Hz, 2H), 7.32 (t, J = 7.6 Hz, 1H), 6.77 (dd, J = 8.5, 2.1 Hz, 1H), 6.72 (s, 1H), 6.25 (d, J = 14.2 Hz, 1H), 4.24 (q, J = 7.3 Hz, 2H), 2.78 (t, J = 6.2 Hz, 2H), 2.72 (t, J = 6.2 Hz, 2H), 2.00 – 1.90 (m, 2H), 1.78 (s, 6H), 1.43 (t, J = 7.2 Hz, 3H). ^{13}C NMR (150 MHz, MeOD) δ 175.91, 164.90, 156.63, 143.08, 139.90, 131.08, 130.97, 129.99, 126.71, 124.49, 123.56, 115.85, 114.96, 112.16, 98.83, 50.82, 40.35, 29.63, 28.64, 21.95, 12.38. HR-MS: calcd for $C_{27}H_{29}N_2O^+$ (M^+):397.2275; found 397.2275.

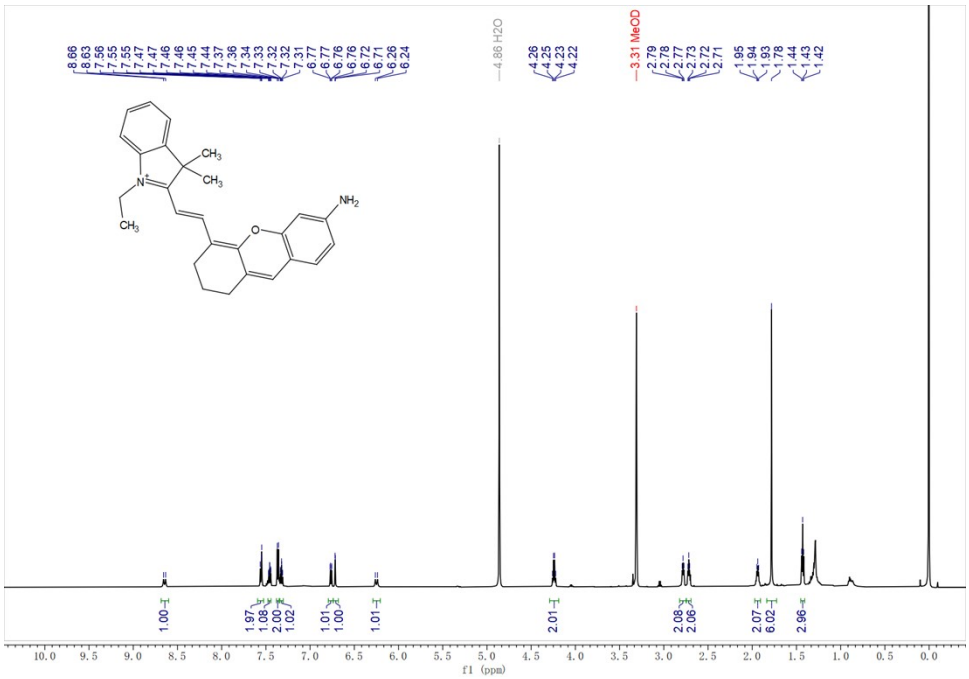

Fig. S3. ^{1}H NMR spectrum of Cy-NH_2.

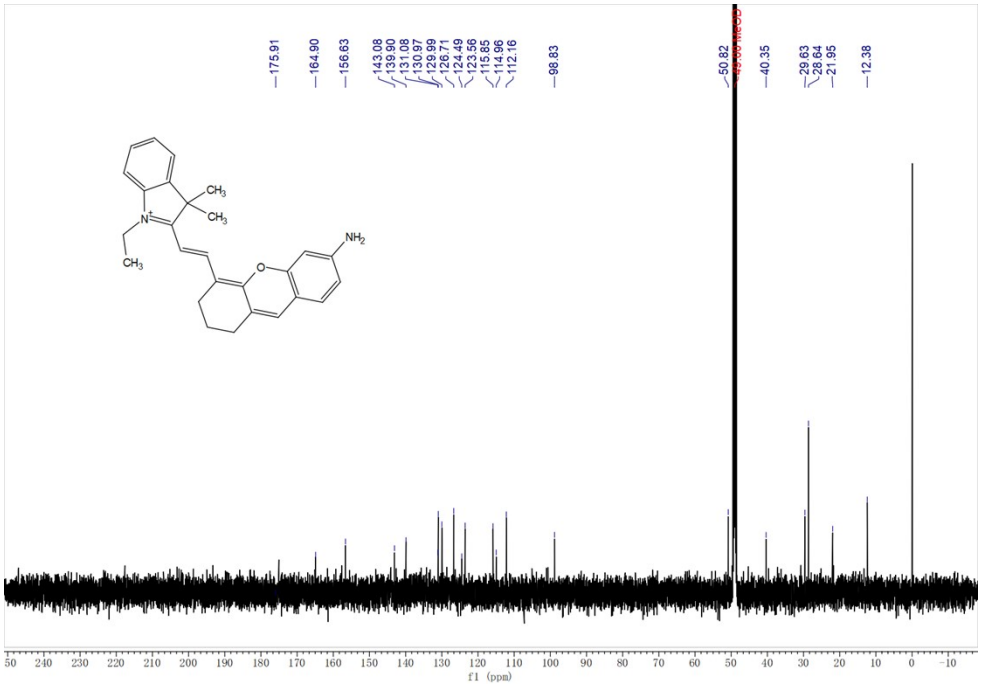

Fig. S4. ^{13}C NMR spectrum of Cy-NH_2.

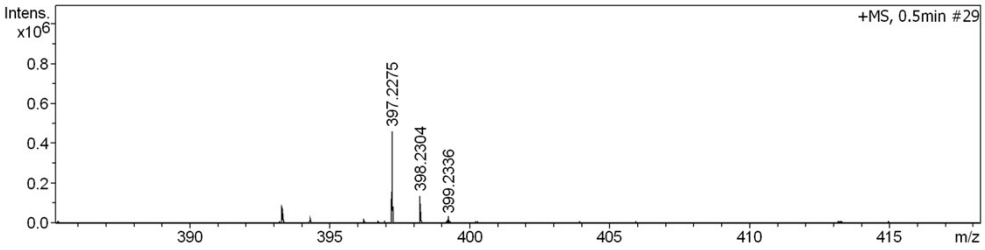

#	m/z	Res.	S/N	I	I %	FWHM
1	397.2275	23890	411.2	459476	100.0	0.0166
2	398.2304	21024	121.1	135184	29.4	0.0189
3	399.2336	21226	20.9	23308	5.1	0.0188

Meas. m/z	#	Ion Formula	m/z	err [ppm]	mSigma		Score	rdb	e¯ Conf	N-Rule
397.2275	1	C27H29N2O	397.2274	-0.2	5.0	1	100.00	14.5	even	ok

Fig. S5. HR-MS spectrum of Cy-NH_2.

Syntheses of Probe Cy-TPE. TPE-2 (376 mg) and Cy-NH_2 (397 mg) were dissolved in 15 mL of ethanol, followed by the addition of three drops of glacial acetic acid as a catalyst. The reaction mixture was stirred at room temperature under a nitrogen atmosphere for 12 hours. After completion, as monitored by TLC, the solvent was removed under reduced pressure using a rotary evaporator. The crude product was purified by column chromatography on silica gel using a mixture of dichloromethane and methanol (10:1, v/v) as the eluent to afford Cy-TPE as a blue solid in 65% yield. ^{1}H NMR (600 MHz, Chloroform-*d*) δ 10.91 (s, 1H), 9.58 (s, 1H), 8.54 (d, *J* = 14.1 Hz, 1H), 7.36 (s, 2H), 7.20–7.17 (m, 2H), 7.12 (t, *J* = 2.6 Hz, 8H), 7.09 (d, *J* = 2.5 Hz, 6H), 7.06–7.02 (m, 4H), 7.01 (t, *J* = 3.7 Hz, 3H), 6.78 (d, *J* = 2.5 Hz, 1H), 6.71 (d, *J* = 9.3 Hz, 1H), 4.10 (d, *J* = 7.3 Hz, 2H), 2.73 (t, *J* = 6.1 Hz, 2H), 2.64 (t, *J* = 6.4 Hz, 2H), 1.97–1.87 (m, 2H), 1.77 (s, 6H), 1.46 (t, *J* = 7.2 Hz, 3H). ^{13}C NMR (150 MHz, $CDCl_3$) δ 196.56, 160.16, 155.45, 143.36, 143.33, 143.03, 141.49, 140.12, 138.87, 136.41, 131.34, 131.26, 131.22, 129.43, 128.64, 128.05, 127.94, 127.74, 126.84, 126.80, 126.64, 125.31, 122.79, 122.31, 120.16, 116.96, 116.06, 110.07, 49.64, 41.04, 29.35, 28.63, 28.57, 28.15, 24.23, 20.74, 12.13. HR-MS: calcd for $C_{54}H_{47}N_2O_2^+$ (M^+):755.3633; found 755.3652.

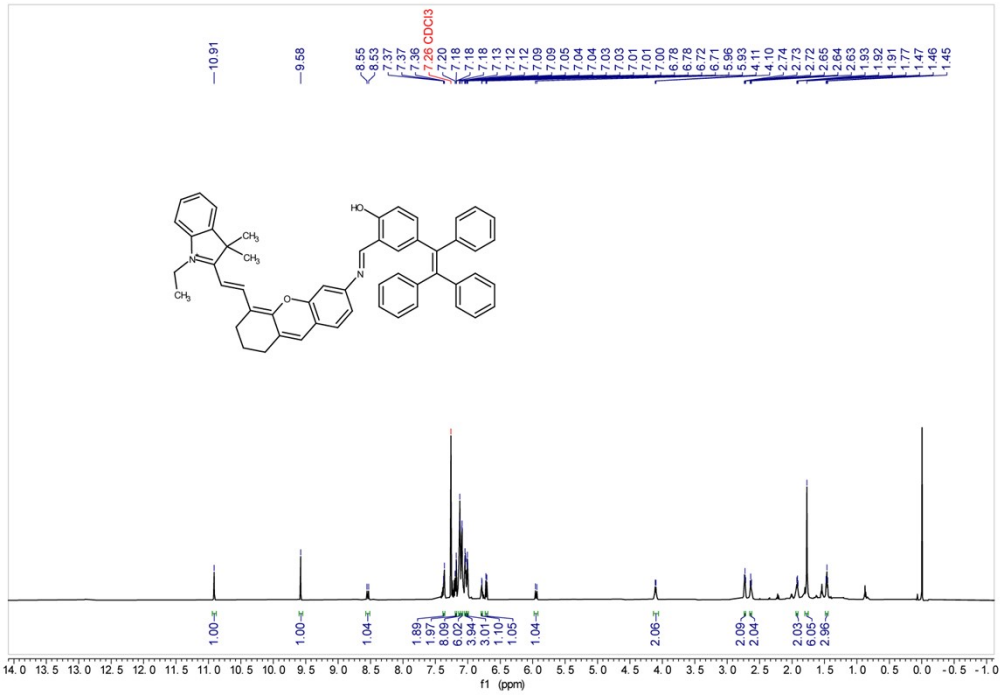

Fig. S6. ^{1}H NMR spectrum of Cy-TPE.

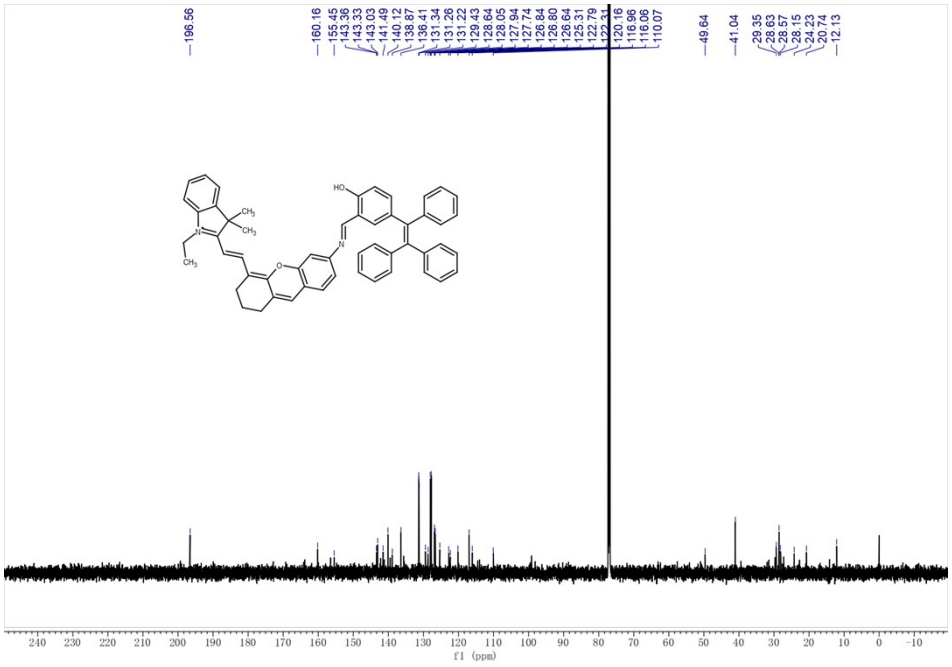

Fig. S7. ^{13}C NMR spectrum of Cy-TPE.

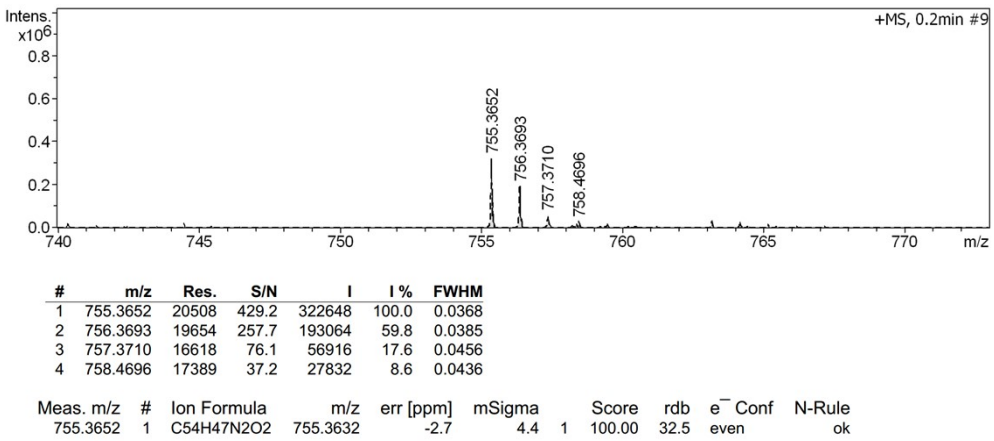

#	m/z	Res.	S/N	I	I %	FWHM
1	755.3652	20508	429.2	322648	100.0	0.0368
2	756.3693	19654	257.7	193064	59.8	0.0385
3	757.3710	16618	76.1	56916	17.6	0.0456
4	758.4696	17389	37.2	27832	8.6	0.0436

Meas. m/z	#	Ion Formula	m/z	err [ppm]	mSigma		Score	rdb	e¯ Conf	N-Rule
755.3652	1	C54H47N2O2	755.3632	-2.7	4.4	1	100.00	32.5	even	ok

Fig. S8. HR-MS spectrum of Cy-TPE.

Table S1. Comparison of reported mitochondrial viscosity probes with Cy-TPE.

Probe structure	λex/λem nm	Viscosity linear range	Bioimaging application	Reference
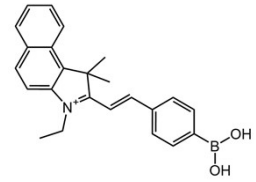	520/593	1-274 cP	Hepatocellular carcinoma cells; tumor-bearing mice	S6
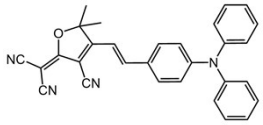	565/654	toluene/DMSO (from 10% to 90%)	HeLa cells	S7
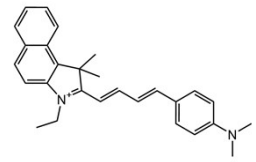	630/700	0.893 to 945 cP	HepG2 cells; pancreatic tissue	S8
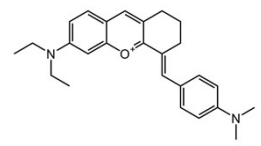	650/740	1-475 cP	HeLa cells	S9
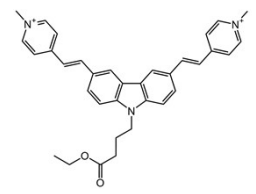	470/550	0.893-435 cP	MCF-7 cells	S10
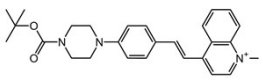	510/667	0.893 to 945 cP	HeLa cells; Mice RA model	S11

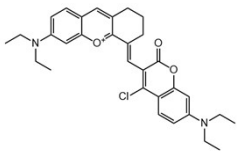	595/722	1.2 to 249 cP	7702 cells, HepG2 cells, PC12 cells and HeLa cells; fatty liver mice.	S12
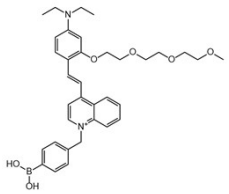	570/670	1.31 to 22.5 cP	OGD/R cell; CIRI rat	S13
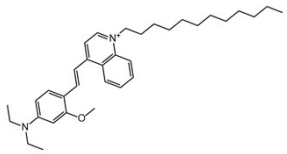	590/665	0.893 to 945 cP	HeLa cells mitophagy process induced by starvation	S14
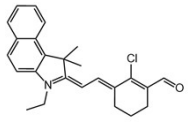	490/635	0.893 to 945 cP	Tumor Theranostics and Apoptosis Imaging	S15
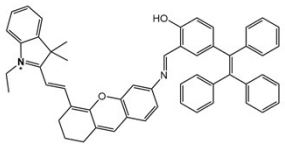	680/725	0.893 to 945 cP	Neuron; epileptic mice	This work

3. Performance Evaluation of Cy-TPE.

Table S2. Photophysical data of Cy-TPE at 25 °C.

Solvent	λ_{abs} (nm)	λ_{em} (nm)	Φ (%)
MeCN	680	720	0.011
DCM	690	725	0.010
THF	700	726	0.009
MeOH	692	724	0.012
H_2O	675	729	0.008
DMF	700	730	0.021
PBS	675	721	0.015
EtOH	699	724	0.013
Diox	705	731	0.035
DMSO	708	730	0.040
Gly	695	720	0.200

[λ_{abs}] Absorption peak. [λ_{em}] Fluorescence emission peak. [Φ] Fluorescence quantum yield: Cy5 [Φ = 0.27 in PBS] was used as a standard.

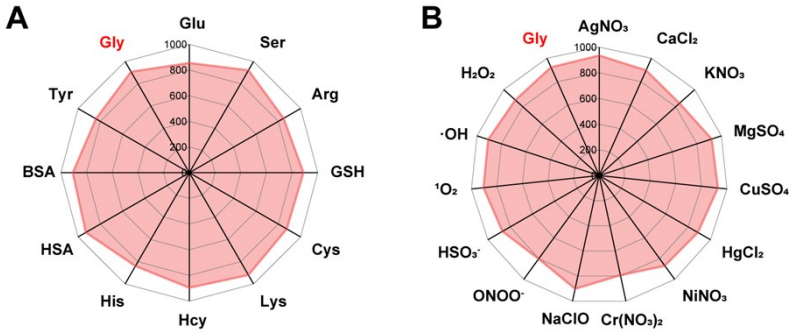

Fig. S9. (A) Fluorescence intensity of Cy-TPE in glycerol in the presence of various biomolecules (100 μM, HSA and BSA 1 mg/mL). (B) Fluorescence intensity of Cy-TPE in glycerol in the presence of various ions and reactive species (100 μM).

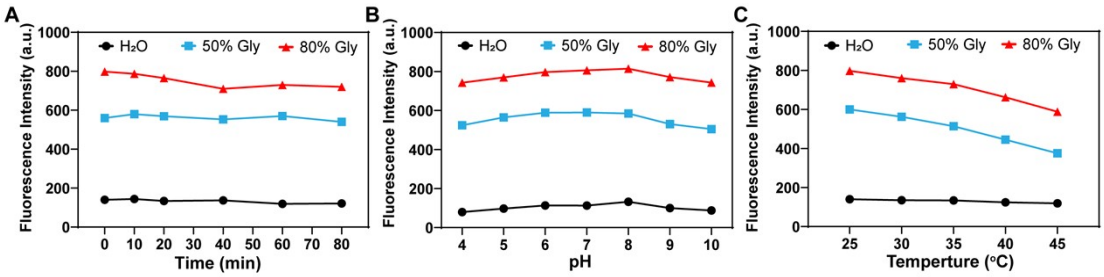

Fig. S10. The effects of (A) reaction time, (B) pH and (C) temperature on the fluorescence intensity of probe Cy-TPE (10 μM) in H_2O and a mixed solution of H_2O, 50% glycerol and 80% glycerol. λex/em = 680 nm/725 nm.

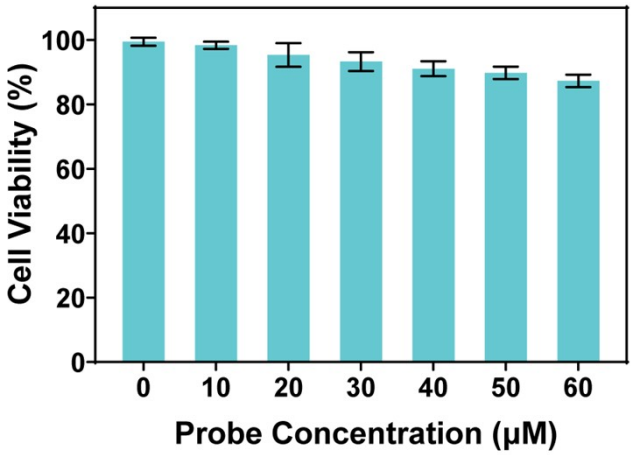

Fig. S11. The CCK-8 assay for neurons upon incubation of Cy-TPE probe with different concentrations (0, 10, 20, 30, 40, 50 and 60 μM) after 24 h, respectively. Error bars: n=5, SEM.

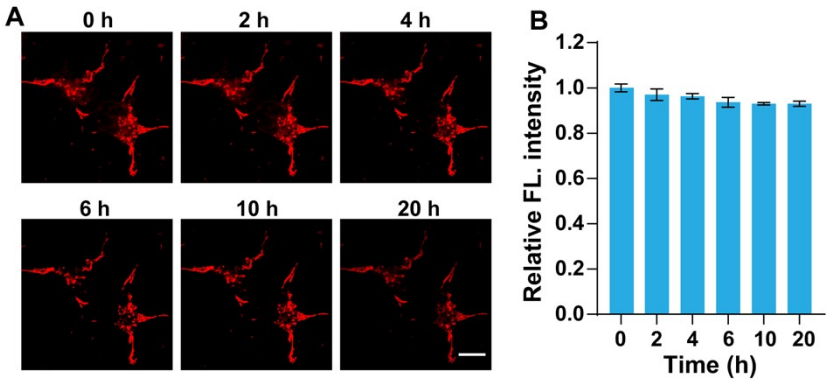

Fig. S12. (A) Fluorescence images of neurons stained with 10 μM Cy-TPE at different time points. (B) The relative fluorescence intensity output of A. Cy-TPE (λex/λem = 680/700-750 nm). Scale bar: 20 μm.

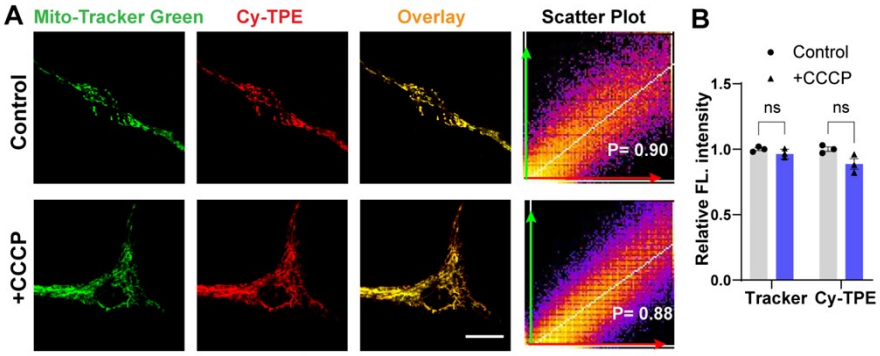

Fig. S13. (A) Co-localization of Mito-Tracker Green (green) with Cy-TPE (red) in neurons without/with CCCP pretreatment (neurons were pretreated with 20 μM CCCP for 10 min, followed by incubation with Mito-Tracker Green and Cy-TPE for 30 min prior to imaging). λex/λem = 680/700-750 nm, Scale bar: 20 μm. (B) Quantification of the relative fluorescence intensity of Mito-Tracker Green and Cy-TPE in control and CCCP-treated neurons. Data are presented as mean ± SEM (n = 3). ***$p < 0.001$; ns, not significant.

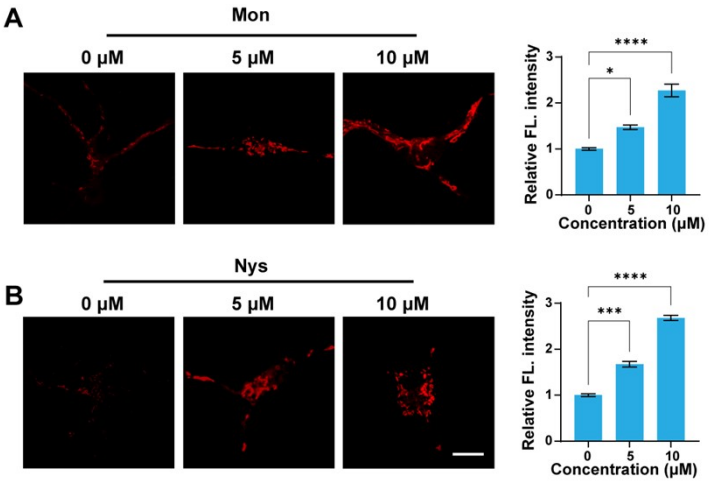

Fig. S14. (A) Neurons were imaged after pretreatment with 0 μM, 5 μM and 10 μM monensin for 30 min, followed by the addition of probe Cy-TPE and incubation for 30 min. (B) Neurons were imaged after pretreatment with 0 μM, 5 μM and 10 μM nystatin for 30 min, followed by the addition of probe Cy-TPE and incubation for 30 min. Relative fluorescence intensity *P<0.1, ***P<0.001, ****P< 0.0001. λex/λem = 680/700-750 nm, Scale bar: 20 μm.

4. Behavioral assessments.

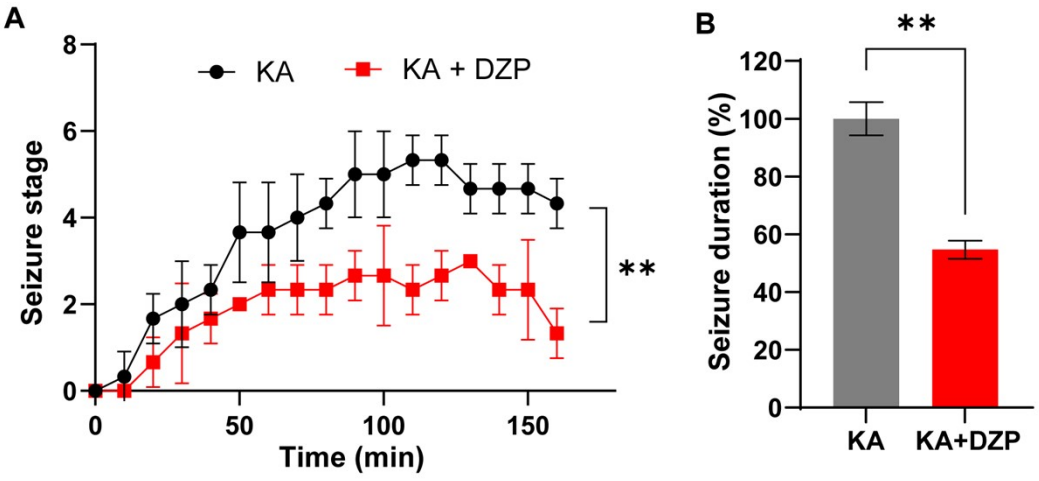

Fig. S15. (A) Seizure stage and (B) Seizure stage duration induced by kainic acid (KA, 20 mg/kg, i.p.) in the presence or absence of diazepam treatment. Error bars: n=5, SEM.

5. References.

S1 T. Lu and F. W. Chen, *J. Comput. Chem*, 2012, **33**, 580-592.

S2 W. Humphrey, A. Dalke and K. Schulten, *J. Mol. Graph. Model.*, 1996, **14**, 33-38.

S3 T. Zhang, F. Yu, H. Xu, M. Chen, X. Chen, L. Guo, C. Zhou, Y. Xu, F. Wang, J. Yu, B. Wu, *Nat. Commun.*, 2021, **12**, 1216.

S4 P. P. Lu, Y. Huang, C. Y. Zhang, L. L. Fu, X. Y. Wang and L. X. Chen, *Talanta*, 2022, **239**, 123111.

S5 S. Y. Liu, H. Xiong, R. R. Li, W. C. Yang and G. F. Yang, *Anal. Chem*., 2019, **91**, 3877-3884.

S6 W. Zhang, Y. Sheng, M. Zhang, Q. Wang, X. Wang, H. Wang, W. Zhang, P. Li and B. Tang, *Chem. Commun.*, 2025, **61**, 13924-13927.

S7 L. Sun, M. Zou, L. Du, S. Wang, R. Ding, K. Lu, J. Li and J. Zhou, *Chem. Commun.*, 2023, **59**, 12735-12738.

S8 B. Chen, S. Mao, Y. Sun, L. Sun, N. Ding, C. Li and J. Zhou, *Chem. Commun.*, 2021, **57**, 4376-4379.

S9 W. Zhang, Y. Lv, H. Song, F. Huo, Y. Zhang and C. Yin, *Chem. Commun.*, 2022, **58**, 8524-8527.

S10 Z. Zou, Q. Yan, S. X. Ai, P. Qi, H. Yang, Y. F. Zhang, Z. H. Qing, L. H. Zhang, F. Feng and R. H. Yang, *Anal. Chem*., 2019, **91**, 8574-8581.

S11 S. Zhang, S. Gong, J. Hong, J. Zhang and G. Feng, *Anal. Chem*., 2025, **97**, 2318-2325.

S12 Y. C. Wu, C. X. Yin, W. J. Zhang, Y. B. Zhang and F. J. Huo, *Anal. Chem*., 2022, **94**, 5069-5074.

S13 C. Fang, Q. Deng, K. C. Zhao, Z. L. Zhou, X. H. Zhu, F. Liu, P. Yin, M. L. Liu, H. T. Li, Y. Y. Zhang and S. Z. Yao, *Anal. Chem*., 2024, **96**, 3436-3444.

S14 J. Hong, X. Guan, Y. Chen, X. Tan, S. Zhang and G. Feng, *Anal. Chem*., 2023, **95**, 5687-5694.

S15 J. Tian, L. Zhang, Y. Qiao, J. Yang, R. Mengji, Y. Lee, S. Hong, Y. Duan, X. Zhou, J. S. Kim and J. Zhou, *Anal. Chem*., 2025, **97**, 15244-15252.